Carbohydrate Polymers 80 (2010) 574–580

Contents lists available at ScienceDirect

Carbohydrate Polymers

journal homepage: www.elsevier.com/locate/carbpol

Short communication

Modifications of alginate-based scaffolds and characterizations of their pentoxifylline release properties

Hsin-Yi Lin [a,b,*], Sin-Yang Ciou [b]

[a] Department of Chemical Engineering and Biotechnology, National Taipei University of Technology, No. 1, Sec. 3, Zhongxiao E. Rd., Taipei 106, Taiwan
[b] Institute of Biotechnology, National Taipei University of Technology, No. 1, Sec. 3, Zhongxiao E. Rd., Taipei 106, Taiwan

ARTICLE INFO

Article history:
Received 23 October 2009
Received in revised form 18 November 2009
Accepted 25 November 2009
Available online 3 December 2009

Keywords:
Alginate
Chitosan
Crosslinking
Controlled release
Anti-inflammation

ABSTRACT

Lyophilized chitosan scaffolds (Cs) and alginate scaffolds crosslinked with calcium (Alg/Ca), chitosan (Alg/Cs), and calcium and chitosan together (Alg/Cs/Ca) were tested for their contact angles, drug release properties, degradability, and compressional moduli. In vitro tests were done to observe how degrees of crosslinking changed the effectiveness of pentoxifylline released from the scaffolds.

Cs had the highest contact angle (83°), followed by Alg/Cs/Ca (70°), Alg/Cs (63°), and Alg/Ca (52°). Alg/Cs/Ca had the highest compressional modulus (9.8 kPa), followed by Alg/Cs (6.3 kPa), Alg/Ca (2.7 kPa) and Cs (2.3 kPa). After 21 days, 2.4% Alg/Cs/Ca degraded in buffered saline while 8.7% of Alg/Ca degraded. The release efficacy of Alg/Cs/Ca was at least 11% less than those of the rest of other scaffolds. In vitro tests showed that activated macrophage cells cultured with Alg/Cs/Ca that released pentoxifylline produced 54–62% less TNF-α and 24–33% less IL-6 compared to cells cultured with other pentoxifylline-releasing scaffolds.

1. Introduction

Alginate is a polyanionic copolymer derived from brown sea algae. It is comprised of 1,4-linked β-D-mannuronic (M) α-L-guluronic (G) residues. Alginate aqueous solution forms stable gels in the presence of certain divalent ions such Ca ions. Alginate beads have been reported to promote phenotype expression (Li, Ramay, Hauch, Xiao, & Zhang, 2005; Li & Zhang, 2005). The anionic property of alginate does not provide a proper microenvironment for fast cell attachment (Pokrywczynska, Drewa, Jundzill, & Lysik, 2008). A cationic polymer such as chitosan can help cell adhesion when added to alginate (Jin, Lee, Park, Park, & Yoon, 2007). Chitosan has been studied as a material for sustained drug release and for use as tissue engineered scaffolds (Chandy & Sharma, 1993; Chung et al., 2002; Illum, 1998; Illum, Jabbal-Gill, Hinchcliffe, Fisher, & Davis, 2001; Olmez, Korkusuz, Bilgili, & Senel, 2007). When mixed with alginate, the opposite charges on chitosan and alginate units form a polyelectrolyte complex. Polyelectrolyte complexes have been used to encapsulate cells and to make devices for controlled drug release (Gåserød, Jolliffe, Hampson, Dettmar, & Skjåk-Bræk, 1998; Kim et al., 1999; Ribeiro, Silva, Ferreira, & Veiga, 2005).

Alginate crosslinked with calcium and/or chitosan have frequently been used to make scaffolds for orthopedic repairs (Jin et al., 2007; Li & Zhang, 2005; Li et al., 2005; Xu et al., 2007;) and skin wound dressings (Goh, Heng, Huang, Li, & Chan, 2008; Kim et al., 2008; Murakami et al., 2010) because of their excellent biocompatibility. Anti-inflammatory medicines have been added to these alginate scaffolds to suppress inflammation in the wound (Işiklan, Inal, & Yigitoglu, 2008; Kulkarni & Sa, 2009; Saxena & Bajpai, 2009). Reduced inflammation around an implant can reduce the chance of implant failure (Revell, 2008). The anti-inflammatory medicines in use have varying strengths and concentrations, which affects how consistently they perform and any side effects that they may cause (Benyamin, Vallejo, Kramer, & Rafeyan, 2008; Cağdaş, Paç, & Cakal, 2008; Dhawan et al., 2009; Rajabalian, Meimandi, & Badinloo, 2009). Hence it is important to characterize the drug release properties of these crosslinked alginate scaffolds. However, to the authors' knowledge, drug release behaviors of the crosslinked alginate scaffolds were never quantitatively studied and compared.

Pentoxifylline (PTX) was used as a model drug in this test. It is an anti-inflammatory drug that has been known to inhibit immune cells from producing inflammatory cytokines as well as to treat or prevent fibrosis (Berman & Duncan, 1989; Berman, Wietzerbin, Sanceau, Merlin, & Duncan, 1992; Pardakhti, Alavi, Kheshti, Eshaghi, & Safaeian, 2009). PTX is known to exert its effects through phosphodiesterase inhibition, resulting in an increase in intracellular levels of cAMP. PTX acts through both protein kinase

* Corresponding author. Address: Department of Chemical Engineering and Biotechnology, National Taipei University of Technology, No. 1, Sec. 3, Zhongxiao E. Rd., Taipei 106, Taiwan. Tel.: +886 2 27712171x2546; fax: +886 2 27317117.
E-mail addresses: hbrunken@ntut.edu.tw, hsin_yi_lin@yahoo.com (H.-Y. Lin), sheepoliver@hotmail.com (S.-Y. Ciou).

0144-8617/$ - see front matter © 2009 Elsevier Ltd. All rights reserved.
doi:10.1016/j.carbpol.2009.11.044

A (PKA) dependent and independent pathways (Costantini et al., 2009). PTX was found to be able to decrease oxidative stress during inflammation and to suppress the superoxide production of macrophage (Bessler, Gilgal, Djaldetti, & Zahavi, 1986; Pardakhti et al., 2009).

To quantify the effects of crosslinking on alginate scaffolds' sustained release properties, alginate and alginate crosslinked with chitosan were made into scaffolds and further crosslinked with Ca ions. Their swelling ratios, pentoxifylline release efficacies, and compressional moduli were measured and compared. The effects of the slow release of PTX on the viability and the inflammatory cytokine release of macrophage cells in vitro are also reported in this study.

2. Materials and methods

2.1. Making alginate and crosslinked alginate films and scaffolds

Chitosan (96 percent deacetylation, 350,000 Da., C&B Co., Taiwan) was dissolved in a 2 v/v% acetic acid solution to make 2 w/v% and 4 w/v% chitosan solutions. Alginate (Acros Organics, NJ, USA) was dissolved in deionized (DI) water to make 2 w/v% and 4 w/v% alginate solutions. Equal volumes of 4 w/v% chitosan and 4 w/v% alginate solutions were stirred together for an hour to make a alginate/chitosan solution. Polymer solutions of 2% alginate, 2% chitosan, and 4% alginate/chitosan were made into films and lyophilized scaffolds. To make films, 1 mL of the polymer solution was coated on the bottom of a polystyrene petri dish (D = 3 cm) and air dried at 25 °C. To make scaffolds, 2 mL of the polymer solution was poured into each glass tube and frozen at −20 °C overnight. The frozen samples were lyophilized in a freeze dryer (RVT4104, Savant, NY, USA).

Alginate films and scaffolds were submerged in 10% $CaCl_2$ aqueous solution overnight (Alg/Ca). Chitosan specimens were neutralized in 0.5 N NaOH and rinsed with DI water (Cs). Alginate/chitosan specimens were neutralized in NaOH and rinsed in DI water (Alg/Cs) and parts of the neutralized Alg/Cs specimens were left in 10% $CaCl_2$ aqueous solution overnight (Alg/Cs/Ca). The specimens were dehydrated in ethanol solutions (from 15%, 50%, 70%, to 95%) and air dried. Films were used for contact angle study while the rest of the tests were done on scaffolds.

2.2. Fourier transform infrared spectrum (FTIR) (n = 3)

To observe whether crosslinking took place, specimens were subjected to FTIR examination. Scaffolds were finely ground, mixed with KBr, and pressed into tabs. The specimens were scanned from 4000 cm^{-1} to 400 cm^{-1} in a FTIR machine (Spectrum Gx, PerkinElmer, MA, USA) with a resolution of 4 cm^{-1}. Transmittance peaks were identified.

2.3. Contact angle (n = 4)

The rate of cell attachment on biomaterials depends largely upon their surface hydrophobicity. Contact angle measurement is an indication of surface hydrophobicity. Five microliters of DI water were placed on each polymer film. Static contact angles were measured using a contact angle meter (CA-D, Kyowa Interface Science Co., Japan).

2.4. Scaffold morphology (n = 3)

Lyophilized scaffolds made of different polymers are known to have different pore sizes and morphologies that affect the scaffolds' capabilities for cell ingrowth and drug release. Dried scaffolds were submerged in liquid nitrogen, sliced, and then sputter coated with gold. A scanning electron microscope (SEM, Hitachi S-3000H, Japan) was used to observe the porous structures of the scaffolds.

2.5. Swelling ratio (n = 3)

A high degree of swelling from an implant is undesirable because it results in lower mechanical strength and a poor fitting to the wound (Anseth, Bowman, & Brannon-Peppas, 1996). After measuring the diameters (D_o) of each dry scaffold (D ~1 cm, h ~0.2 cm), the scaffolds were placed in phosphate buffered saline (PBS, pH 7.4) and their diameters were measured at each designated time point (D_t). The swelling ratio at each time point was calculated as $[(D_t - D_o)/D_o] \times 100\%$.

2.6. Release efficiency (n = 3)

Compared to most biomaterials, hydrogels often have high degradability in the liquid phase and high initial drug release rates, which result in an undesirable high drug concentration in surrounding tissues. Hydrogels also have low mechanical strength for most tissue repair purposes. The four kinds of lyophilized scaffolds in this study were tested for the above properties.

Each dry scaffold disc (D ~1 cm, h ~0.2 cm) was evenly loaded with 50 μL of pentoxifylline (PTX, 20 mg/ml) and left to dry at room temperature overnight. Ten scaffold discs were placed in each beaker filled with 100 mL of PBS and there were three beakers (n = 3) for each polymer. All beakers were placed on a shaker (50 rpm) during the test. At each designated time point, 100 μL of PBS was sampled, and the same volume of PBS was replenished. The absorbance of PTX at 274 nm was measured (Gene Quant 1300 spectrophotometer, GE Healthcare, NJ) and converted to concentrations (M_t (μg/mL)). The release efficiency of the PTX was calculated as $[(M_t\ /100\ \mu g/mL)] \times 100\%$. After the PTX in the ten scaffolds were released, the final PTX concentration in each beaker was 100 μg/mL.

2.7. Degradation (n = 3)

A scaffold with an initial dry weight of W_o was placed in a 15 mL centrifuge tube filled with 5 mL of PBS (pH 7.4). The tubes were placed in an incubator (37 °C) and the lysozyme solution was changed every 3 days. After 3 weeks, three tubes of each specimen were removed from the incubator and the remaining scaffolds were rinsed carefully several times with DI water and air dried to obtain their dry weights (W). The percentage of weight loss was calculated as $[(W_o - W)/W_o] \times 100\%$.

2.8. Compression (n = 4)

Dry scaffolds (D ~1 cm; h ~1.2 cm) were submerged in PBS overnight and any excess liquid was removed before testing. A Universal Micro-tribometer (model UMT-2, CETR, CA, USA) was used to obtain stress–strain curves. The exact diameters and heights of each scaffold were measured right before the test. The speed of the crosshead was 0.3 mm/s and a 10 N load cell was used. The test stopped at 80% strain. The slope of the initial linear section of the stress–strain curve was used to estimate the Young's modulus.

2.9. Effects of PTX on cell proliferation, viability, TNF-α and IL-6 release (n = 4)

Macrophage cells (RAW 264.7, ATCC, VA) were cultured in DMEM (Invitrogen, CA, USA) with 10% fetal bovine serum, 100 U/mL penicillin, and 100 μg/mL streptomycin. They were kept in a cell culture

incubator (SCA-165DS, ASTEC, Japan) at 37 °C with 95% humidity and 5% CO_2. Cells were seeded onto 24-well tissue culture plates (TCPs, BD Biosciences, CA) at $1 \times 10^5/cm^2$ and allowed to settle overnight in the incubator. Medium was then removed from each well and replenished with 2 mL fresh media or media with 1 μg/ml lipopolysaccharide (LPS). LPS was used to activate the macrophage cells to release inflammatory factors (Lin & Bumgardner, 2004). Scaffolds were submerged in 70% ethanol and exposed to UV briefly before being rinsed in sterile PBS. Excess PBS was then removed and 10 μL of pentoxifylline (20 mg/ml) was added to each scaffold. Cells were then separated into the groups listed in Table 1.

At 6 and 24 h, culture medium from each well was collected and kept at −80 °C for later analyses of tumor necrosis factor alpha (TNF-α) and interleukin 6 (IL-6). To estimate cell numbers, cells at the bottom of each well were scraped off using a cell scraper (Bio-One, Greiner, NC, USA) and stained with trypan blue. Live cells were counted using a hemocytometer. To measure cell viability, culture medium was removed, and the wells were rinsed with PBS. Half a milliliter of MTT (3-(4,5)-dimethylthiahiazo(-z-yl)-3,5-di-phenytetrazoliumromide, 1 mg/mL) was added to each well. Four hours later, MTT was removed and 300 μL of isopropanol was added to extract the purple formazan dye. Absorbance at 570 nm was measured using a multi-well spectrophotometer (Sunrise, TECAN, Switzerland).

The TNF-α and IL-6 in the media were measured using commercial kits (Mouse TNF-α ELISA OptiEIA, BD Bioscience, CA, and Mouse IL-6 ELISA DuoSet, R&D, MN).

Table 1
In vitro cell culture conditions for testing of effects of PTX on macrophage cells when PTX was released from scaffolds into the culture media. Items that were added or absent in culture media are marked with + and −, respectively.

Test condition symbols	LPS	PTX	Blank scaffold	Scaffold with 0.2 mg PTX(*)
TCP	−	−	−	−
(†)	−	+	−	−
(‡)	−	−	+	−
TCP + LPS	+	−	−	−
TCP + LPS + PTX	+	+	−	−
(&)	+	−	+	−
TCP+LPS+PTX release from scaffolds	+	−	−	+

* Final concentration in each well with 2 mL medium was 100 μL/mL.
†,‡,& Results are not be shown in figures.

2.10. Statistical analysis

All data is presented as an average ± standard deviation. Statistical analysis was conducted using one- way ANOVA with Tukey tests (SigmaStat 3.5 for Windows, Systat Software, IL). The difference between alginate-crosslinked chitosan and chitosan was declared when $p < 0.05$.

3. Results and discussion

3.1. FT-IR

Alginate, an anionic polysaccharide, forms a polyelectrolyte complex with chitosan, a cationic polysaccharide, through the ionic attraction between the NH_3^+ group in chitosan and the COO^- group in alginate (Chung et al., 2002; Takahashi, Takayama, Machida, & Nagai, 1990; Li et al., 2005). When alginate-containing scaffolds were submerged into a solution containing Ca ions, the negatively charged carboxyl (COO^-) groups on alginate molecules are drawn to Ca ions.

The FT-IR spectra of Alg/Ca, Alg/Cs, Alg/Cs/Ca, and Cs are not shown for they are similar to previously published results (Li et al., 2005). The FT-IR spectra showed that alginate formed polyelectrolyte complex with chitosan and with calcium. When Alg/Cs complex was further crosslinked in a calcium solution, Ca

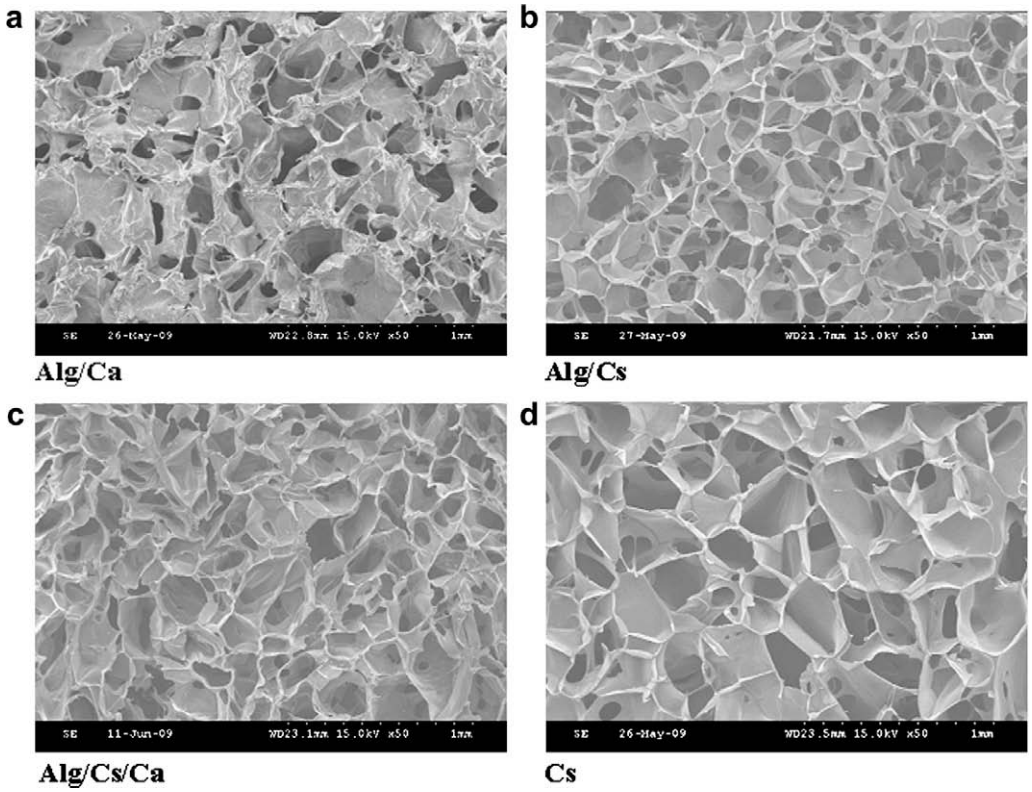

Fig. 1. Representative SEM microphotographs of (a) Alg/Ca, (b) Alg/Cs, (c) Alg/Cs/Ca, (d) Cs scaffolds. Scale bar = 1 mm for all micrographs.

ions interacted with residual carboxyl groups on alginate and coacervated into another network.

3.2. Contact angle

The contact angles of Alg/Ca, Alg/Cs, Alg/Cs/Ca, and Cs were 51.6 ± 3.9, 63.1 ± 2.7, 70.1 ± 2.5, and 82.8 ± 3.1, respectively. Alginate is water soluble in DI water while chitosan is not. Hence, the addition of chitosan to alginate made alginate less hydrophilic. Alg/Cs became more hydrophobic after residual alginate was crosslinked with Ca ions. This is due to the high carboxylate functionality of alginate, as well as the excess of carboxylate functionality expected at the surface of a pure polyamide composite membrane (Jin, Huang, & Hoek, 2009).

3.3. SEM

SEM micrographs showed that Alg/Ca had irregular pore morphology, and most of its pores were closed compared to others (Fig. 1). Cs had the largest pores with defined outlines compared to others. Alg/Cs and Alg/Cs/Ca had smaller pores than Cs because they were made from a higher concentration of (4 w/v%) polymer solution than Cs (2 w/v%). Chung et al. (2002) reported decreased porosity and pore size after chitosan was crosslinked with alginate. The polyelectrolyte complex and ionic bonds between the two polymers were thought to result in a less porous structure as well (Chung et al., 2002; Madihally & Matthew, 1999).

3.4. Swelling ratio

At 90 min, Cs had the highest swelling ratio, followed by Alg/Cs, and then Alg/Cs/Ca. Alg/Ca had the lowest swelling ratio (Fig. 2). Alg/Ca and Alg/Cs/Ca had initial bursts in swelling within several seconds and their swelling quickly reached equilibrium. The swelling ratios of Alg/Cs and Cs reached their maximum values in a more gradual way.

A scaffold's swelling property depends largely on its porosity and pore size and partly on the material's wettability (Kim, Park, Kim, Wada, & Kaplan, 2005). Cs had the largest pore size of all (Fig. 1) and therefore the highest swelling ratio. Alg/Cs and Alg/Cs/Ca had similar pore sizes, but Alg/Cs had a higher wettability (lower contact angle) than Alg/Cs/Ca. As a result, Alg/Cs had higher swelling ratios than Alg/Cs/Ca. The reason Alg/Ca had the lowest swelling ratio was, based on the authors' observations, that Alg/Ca scaffolds shrunk very little during the ethanol dehydrating process. With its high wettability, Alg/Ca scaffolds quickly expanded to their original sizes when rehydrated.

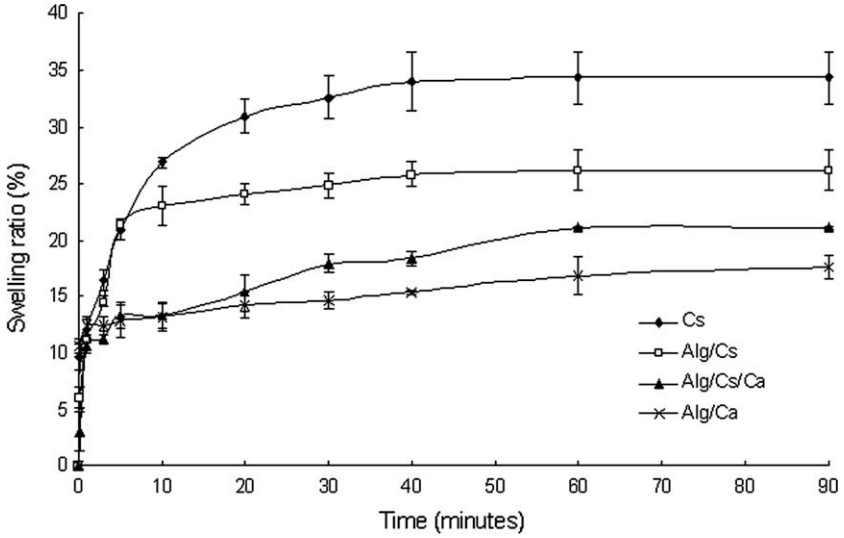

Fig. 2. The swelling ratios of Alg/Ca, Alg/Cs, Alg/Cs/Ca, and Cs scaffolds.

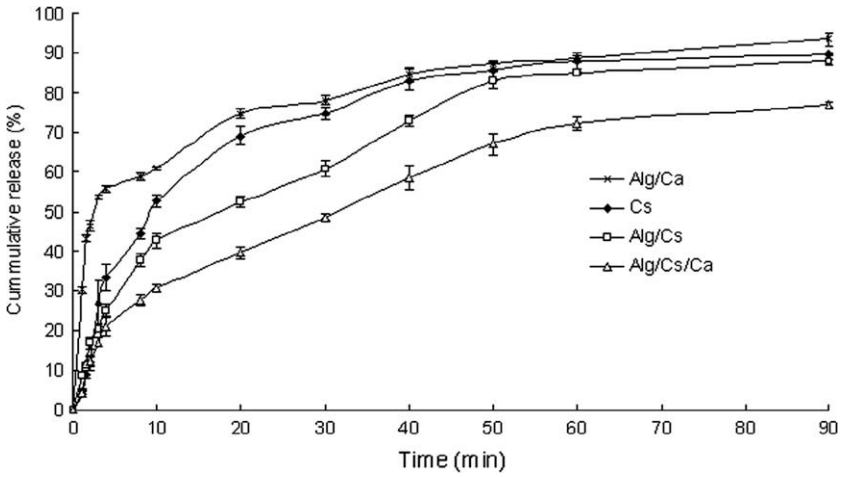

Fig. 3. The pentoxifylline release efficacies of Alg/Ca, Alg/Cs, Alg/Cs/Ca, and Cs scaffolds.

3.5. Release efficacy

PTX was most quickly released from Alg/Ca with an initial burst of over 50% PTX release in less than 5 min (Fig. 3). Cs scaffolds had a much lower initial burst but similar total PTX release after 40 min compared to Alg/Ca. After alginate and chitosan formed polyelectrolyte complexes (Alg/Cs and Alg/Cs/Ca), the initial burst of PTX significantly decreased compared to chitosan and alginate alone. The amounts of PTX released from Alg/Ca, Cs, and Alg/Cs were similar at 90 min. Alg/Cs/Ca had a 10–16% lower release efficacy compared to other scaffolds.

Release efficacy of a hydrogel is mostly influenced by diffusion and swelling (Pasparakis & Bouropoulos, 2006). When the swelling ratio of a hydrogel reaches a constant, it stops influencing the release efficacy. The diffusion efficiency of a drug inside a hydrogel depends largely on the polymer mass density and the degree of crosslinking. Alg/Ca and Cs scaffolds had half of the polymer mass of Alg/Cs and Alg/Cs/Ca and thus higher PTX release rates. Alg/Ca reached its maximum swelling ratio faster than Cs did, and hence it had a greater release efficacy than Cs. Alg/Cs/Ca had a similar polymer mass as Alg/Cs but was further crosslinked with Ca ions. Crosslinking reduced the diffusion efficiency of alginate (Pasparakis & Bouropoulos, 2006) and thus the release efficacy of alginate hydrogel as well.

3.6. Degradation

After 3 weeks, the amount of weight loss (%) from Alg/Ca, Cs, Alg/Cs, and Alg/Cs/Ca was 8.7 ± 0.4, 4.9 ± 0.4, 4.3 ± 0.6, and 2.4 ± 0.3, respectively. Alginate is soluble in water, but ionic binding with Ca ions makes it insoluble. In PBS, an abundant amount of Na^+ ions gradually replaced Ca ions in the Alg/Ca network (Bajpai & Sharma, 2004). Na^+ has only one positive charge and does not induce alginate gelation. Without crosslinking, Alg/Ca gradually dissolved back into the aqueous phase. Cs had a higher degradation rate than Alg/Cs and Alg/Cs/Ca due to its lower initial dry weight and its high swelling ratio which allowed for greater water entry. The stability of alginate increased after forming a polyelectrolyte with cationic compounds such as chitosan and calcium (Murata, Miyamoto, & Kawashima, 1996; Takeuchi, Yasuji, Yamamoto, & Kawashima, 2000). As a result, Alg/Cs/Ca is more resistant to hydrolysis than Alg/Cs.

3.7. Compressional Young's modulus

Young's modulus (E) is an indication of a material's stiffness. Alg/Ca (E = 2.7 ± 0.5 kPa) and Cs (E = 2.3 ± 0.2 kPa) scaffolds had similar Young's moduli ($p > 0.1$). The moduli of Alg/Cs (E = 6.3 ± 0.5 kPa) and Alg/Cs/Ca (E = 9.9 ± 0.7 kPa) were two to four times higher than those of Alg/Ca and Cs. Bartkowiak and Hunkeler (2000) found that the mechanical properties of alginate beads depend on the polymer's molecular mass and the concentration of the polymer in the solution. The higher the molecular mass and the concentration of alginate in the solution, the stiffer the alginate beads are. That study agrees with our results that Alg/Cs and Alg/Cs/Ca (made from 4 w/v% polymer solution) were stiffer than Alg/Ca and Cs (made from 2 w/v% polymer solution). The presence of Ca ions in a solution induces the formation of strong bridges between alginate molecules. The complexation through Ca ions between alginate units allows the matrix to stretch further until the polymers are broken free by external forces (de Kerchove & Elimelech, 2007).

Li et al. (2005) did compressional test on *dry* scaffolds made of chitosan and alginate–calcium-crosslinked chitosan. The concentrations of chitosan and alginate used in their study were 1.6–5 times higher than those used in our study. They reported chitosan and alginate–calcium-crosslinked chitosan scaffolds having Young's moduli of 2.56 MPa and 8.16 MPa, respectively.

3.8. Effects of PTX on cell proliferation, viability, TNF-α and IL-6 release

When macrophages were cultured in DMEM with PTX (100 μg/mL and 200 μg/mL) for 24 h (condition † in Table 1), their

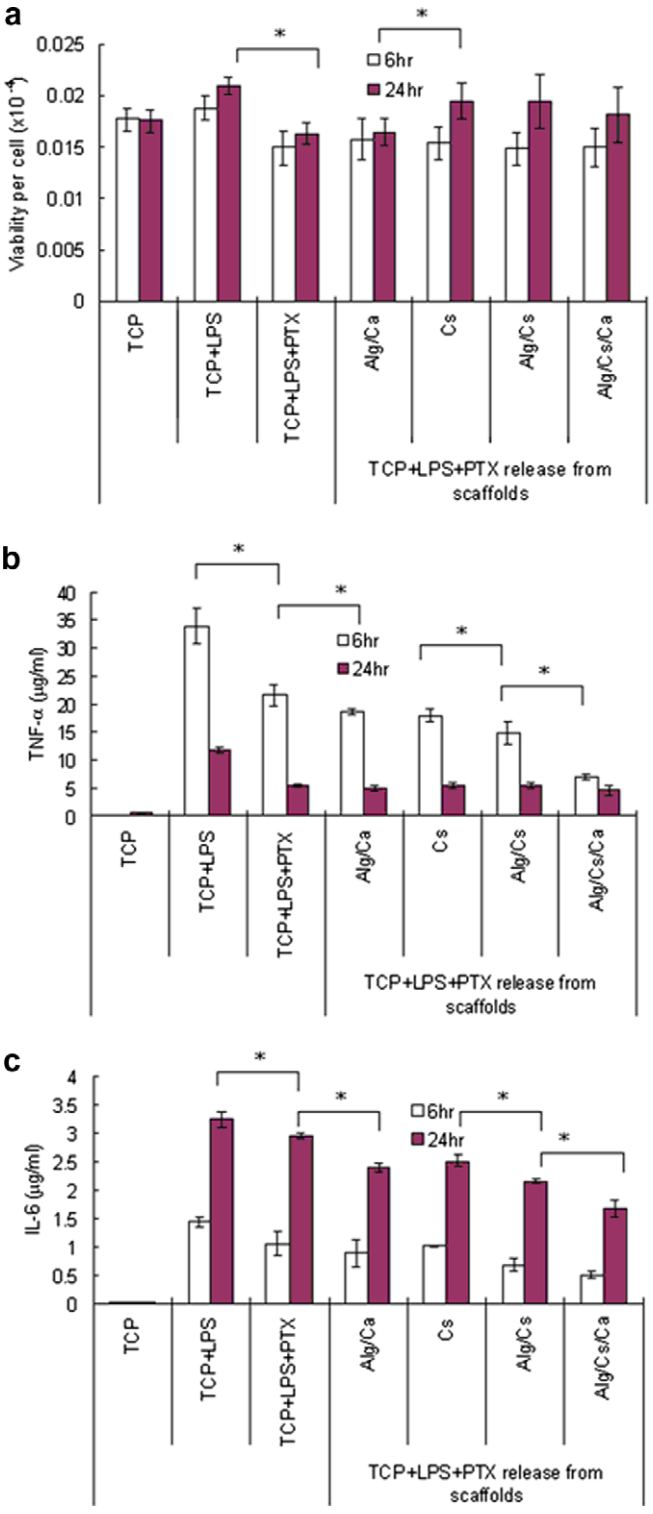

Fig. 4. Macrophage cell viability (a), TNF-α (b) and IL-6 (c) accumulations at 6 h and 24 h under the conditions in Table 1. *: statistical difference ($p < 0.05$) exists between two groups.

viabilities were reduced to 70% and 50%, respectively, of that of TCP control (no PTX added). Further tests were conducted using 100 μg/mL of PTX to avoid significant cell death.

The presence of blank scaffolds did not alter the viabilities of macrophage cells (conditions ‡ and & in Table 1) compared to controls (no scaffold present). The amounts of TNF-α and IL-6 released from non-activated macrophage cells cultured with blank scaffolds (‡ in Table 1) were negligible. The amounts of TNF-α and IL-6 released from activated macrophage cells cultured with the four kinds of scaffolds (condition & in Table 1) were similar at six hours and 24 h.

The effects of the PTX release rate on a macrophage's viability and TNF-α and IL-6 production are shown in Fig. 4. When PTX was added directly to the medium with activated cells, the cell viability decreased at both 6 h and 24 h (Fig. 4(a)) compared to the control without the addition of PTX. However, when PTX was slowly released from scaffolds into medium, the cells' viabilities were as high as the control (except for Alg/Ca group) at 24 h. The slow release of PTX seemed to have less of an adverse effect on macrophage cells.

The amount of TNF-α released from activated cells decreased from 6 h to 24 h. At 24 h, all test groups had a similar TNF- α level (~5 μg/ml).

The following discussion of TNF-α release is based on data from 6 h. For activated macrophage cells, the addition of PTX into the medium reduced the amount of TNF-α released (Fig. 4(b)). The TNF-α release was further reduced when PTX in medium was slowly released from scaffolds. The amount of TNF- α released was inversely proportional to the PTX release rates. Compared to cells cultured in medium with direct PTX addition, cells in the Alg/Cs/Ca group released 68% less TNF-α at 6 h.

The amount of IL-6 released from activated macrophages increased from 6 h to 24 h. Discussion here is based on numbers from 24 h in Fig. 4(c). The cells released less IL-6 after PTX was directly added to the medium. Cells released even less IL-6 when PTX was slowly released into medium from scaffolds. Similar to TNF-α, the amount of IL-6 released was inversely proportional to PTX release efficacies.

At the dosage of 100 μg/ml, PTX is known to suppress immune cell proliferation (Bruynzeel, Stoof, & Willemze, 1998; Vukanic, Colic, and Dimitrijevic, 2007). Based on the three possible cellular metabolic pathways of PTX (Costantini et al., 2009), it is speculated that when a high dosage of PTX was added to macrophage cells in this test, it was used not only in suppressing TNF-α mRNA and the sequential IL-6 expressions, but also in inhibiting cell proliferation (Vukanic et al., 2007). Therefore, PTX was being used in several metabolic pathways at higher concentrations. However, when PTX was slowly provided to macrophage cells, a low, yet effective, concentration of PTX (<10 μg/ml) (Vukanic et al., 2007) could be achieved that suppressed TNF-α expression, but not cell growth or superoxide production. Kofuji et al. (2004) implanted chitosan beads retaining the anti-inflammatory drug prednisolone (PS) into the back of mice. They found inflammation significantly reduced after implantation of chitosan beads when compared with the injection of a PS suspension. They concluded that sustained PS release provides a minimum effective dose for prolonged periods, while with a direct injection most of the PS is removed in the process of diffusion because of the high concentration gradient.

4. Summary

Our results showed that crosslinking with calcium and chitosan changed the properties and porous structures of the lyophilized alginate scaffolds. In general, the more crosslinked a alginate scaffold was, the stronger and more stable it became and the more suitable it was to be a controlled release carrier.

Acknowledgement

This project is funded mainly by grants from the National Science Council: NSC 97-2221-E-027-001.

References

Anseth, K. S., Bowman, C. N., & Brannon-Peppas, L. (1996). Mechanical properties of hydrogels and their experimental determination. *Biomaterials, 17*, 1647–1657.

Bajpai, S. K., & Sharma, S. (2004). Investigation of swelling/degradation behaviour of alginate beads crosslinked with Ca^{2+} and Ba^{2+} ions. *Reactive and Functional Polymers, 59*, 129–140.

Bartkowiak, A., & Hunkeler, D. (2000). Alginate–oligochitosan microcapsules. II. Control of mechanical resistance and permeability of the membrane. *Chemistry of Materials, 12*, 206–212.

Benyamin, R. M., Vallejo, R., Kramer, J., & Rafeyan, R. (2008). Corticosteroid induced psychosis in the pain management setting. *Pain Physician, 11*, 917–920.

Berman, B., & Duncan, M. R. (1989). Pentoxifylline inhibits normal human dermal fibroblast in vitro proliferation, collagen, glycosaminoglycan, and fibronectin production, and increases collagenase activity. *Journal of Investigative Dermatology, 92*, 605–610.

Berman, B., Wietzerbin, J., Sanceau, J., Merlin, G., & Duncan, M. R. (1992). Pentoxifylline inhibits certain constitutive and tumor necrosis factor-α induced activities of human normal dermal fibroblasts. *Journal of Investigative Dermatology, 98*, 706–712.

Bessler, H., Gilgal, R., Djaldetti, M., & Zahavi, I. (1986). Effect of pentoxifylline on the phagocytic activity, cAMP levels, and superoxide anion production by monocytes and polymorphonuclear cells. *Journal of Leukocyte Biology, 40*, 747–754.

Bruynzeel, I., Stoof, T. J., & Willemze, R. (1998). Pentoxifylline and skin inflammation. *Clinical and Experimental Dermatology, 23*, 168–172.

Cağdaş, D. N., Paç, F. A., & Cakal, E. (2008). Glucocorticoid-induced diabetic ketoacidosis in acute rheumatic fever. *Journal of Cardiovascular Pharmacology and Therapeutics, 13*, 298–300.

Chandy, T., & Sharma, C. P. (1993). Chitosan matrix for oral sustained delivery of ampicillin. *Biomaterials, 14*, 939–944.

Chung, T. W., Yang, J., Akaike, T., Cho, K. Y., Nah, J. W., Kim, S. I., et al. (2002). Preparation of alginate/galactosylated chitosan scaffold for hepatocyte attachment. *Biomaterials, 23*, 2827–2834.

Costantini, T. W., Deree, J., Loomis, W., Putnam, J. G., Choi, S., Baird, A., et al. (2009). Phosphodiesterase inhibition attenuates alterations to the tight junction proteins occludin and ZO-1 in immunostimulated Caco-2 intestinal monolayers. *Life Sciences, 84*, 18–22.

de Kerchove, A. J., & Elimelech, M. (2007). Formation of polysaccharide gel layers in the presence of Ca^{2+} and K^{+} ions: Measurements and mechanisms. *Biomacromolecules, 8*, 113–121.

Dhawan, N., Das, S., Kiran, U., Chauhan, S., Bisoi, A. K., & Makhija, N. (2009). Effect of rectal diclofenac in reducing postoperative pain and rescue analgesia requirement after cardiac surgery. *Pain Practice, 9*, 385–393.

Gåserød, O., Jolliffe, I. G., Hampson, F. C., Dettmar, P. W., & Skjåk-Bræk, G. (1998). The enhancement of the bioadhesive properties of calcium alginate gel beads by coating with chitosan. *International Journal of Pharmaceutics, 175*, 237–246.

Goh, C. H., Heng, P. W. S., Huang, E. P. E., Li, B. K. H., & Chan, L. W. (2008). Interactions of antimicrobial compounds with cross-linking agents of alginate dressings. *Journal of Antimicrobial Chemotherapy, 62*, 105–108.

Illum, L. (1998). Chitosan and its use as a pharmaceutical excipient. *Pharmaceutical Research, 15*, 1326–1331.

Illum, L., Jabbal-Gill, I., Hinchcliffe, M., Fisher, A. N., & Davis, S. S. (2001). Chitosan as a novel nasal delivery system for vaccines. *Advanced Drug Delivery Reviews, 51*, 81–96.

Işiklan, N., Inal, M., & Yigitoglu, M. (2008). Synthesis and characterization of poly(*N*-vinyl-2-pyrrolidone) grafted sodium alginate hydrogel beads for the controlled release of indomethacin. *Journal of Applied Polymer Science, 110*, 481–493.

Jin, X., Huang, X., & Hoek, E. M. (2009). Role of specific ion interactions in seawater RO membrane fouling by alginic acid. *Environmental Science and Technology, 43*, 3580–3587.

Jin, H.-H., Lee, H.-M., Park, I.-M., Park, H.-C., & Yoon, S.-Y. (2007). Preparation of macroporous hydroxyapatite/chitosan-alginate composite scaffolds for bone implants. *Key Engineering Materials, 342–343*, 217–220.

Kim, H.-J., Lee, H.-C., Oh, J.-S., Shin, B.-A., Oh, C.-S., Park, R.-D., et al. (1999). Polyelectrolyte complex composed of chitosan and sodium alginate for wound dressing application. *Journal of Biomaterials Science, Polymer Edition, 10*, 543–556.

Kim, J. O., Park, J. K., Kim, J. H., Jin, S. G., Yong, C. S., Li, D. X., et al. (2008). Development of polyvinyl alcohol–sodium alginate gel–matrix-based wound dressing system containing nitrofurazone. *International Journal of Pharmaceutics, 359*, 79–86.

Kim, U.-J., Park, J., Kim, H.-J., Wada, M., & Kaplan, D. L. (2005). Three-dimensional aqueous-derived biomaterial scaffolds from silk fibroin. *Biomaterials, 26*, 2775–2785.

Kofuji, K., Akamine, H., Qian, C. J., Watanabe, K., Togan, Y., Nishimura, M., et al. (2004). Therapeutic efficacy of sustained drug release from chitosan gel on local inflammation. *International Journal of Pharmaceutics, 272*, 65–78.

Kulkarni, R. V., & Sa, B. (2009). Polyacrylamide-grafted-alginate-based pH-sensitive hydrogel beads for delivery of ketoprofen to the intestine: In vitro and in vivo evaluation. *Journal of Biomaterials Science, Polymer Edition, 20*, 235–251.

Li, Z., Ramay, H. R., Hauch, K. D., Xiao, D., & Zhang, M. (2005). Chitosan-alginate hybrid scaffolds for bone tissue engineering. *Biomaterials, 26*, 3919–3928.

Li, Z., & Zhang, M. (2005). Chitosan-alginate as scaffolding material for cartilage tissue engineering. *Journal of Biomedical Materials Research Part A, 75*, 485–493.

Lin, H., & Bumgardner, J. D. (2004). In vitro biocorrosion of Co–Cr–Mo implant alloy by macrophage cells. *Journal of Orthopaedic Research, 22*, 1231–1236.

Madihally, S. V., & Matthew, H. W. (1999). Porous chitosan scaffolds for tissue engineering. *Biomaterials, 20*, 1133–1142.

Murakami, K., Aoki, H., Nakamura, S., Nakamura, S.-I., Takikawa, M., Hanzawa, M., et al. (2010). Hydrogel blends of chitin/chitosan, fucoidan and alginate as healing-impaired wound dressings. *Biomaterials, 31*, 83–90.

Murata, Y., Miyamoto, E., & Kawashima, S. (1996). Additive effect of chondroitin sulfate and chitosan on drug release from calcium-induced alginate gel beads. *Journal of Controlled Release, 38*, 101–108.

Olmez, S. S., Korkusuz, P., Bilgili, H., & Senel, S. (2007). Chitosan and alginate scaffolds for bone tissue regeneration. *Pharmazie, 62*, 423–431.

Pardakhti, A., Alavi, S. A., Kheshti, N. M., Eshaghi, P., & Safaeian, L. (2009). Effect of slow release pentoxifylline and captopril on delayed pulmonary complications of mustard gas in animal models. *Tanaffos, 8*, 41–49.

Pasparakis, G., & Bouropoulos, N. (2006). Swelling studies and in vitro release of verapamil from calcium alginate and calcium alginate–chitosan beads. *International Journal of Pharmaceutics, 323*, 34–42.

Pokrywczynska, M., Drewa, T., Jundzill, A., & Lysik, J. (2008). Alginate is not a good material for growth of rapidly proliferating cells. *Transplantation Proceedings, 40*, 1664–1667.

Rajabalian, S., Meimandi, M. S., & Badinloo, M. (2009). Diclofenac inhibits proliferation but not NGF-induced differentiation of PC12 cells. *Pakistan Journal of Pharmaceutical Scienes, 22*, 259–262.

Revell, P. A. (2008). The combined role of wear particles, macrophages and lymphocytes in the loosening of total joint prostheses. *Journal of the Royal Society Interface, 5*, 1263–1278.

Ribeiro, A. J., Silva, C., Ferreira, D., & Veiga, F. (2005). Chitosan-reinforced alginate microspheres obtained through the emulsification/internal gelation technique. *European Journal of Pharmaceutical Sciences, 25*, 31–40.

Saxena, S., & Bajpai, S. K. (2009). Controlled delivery of diclofenac sodium from calcium alginate beads loaded with a drug-resin complex. *Journal of Applied Polymer Science, 112*, 416–424.

Takahashi, T., Takayama, K., Machida, Y., & Nagai, T. (1990). Characteristics of polyion complexes of chitosan with sodium alginate and sodium polyacrylate. *International Journal of Pharmaceutics, 61*, 35–41.

Takeuchi, H., Yasuji, T., Yamamoto, H., & Kawashima, Y. (2000). Spray-dried lactose composite particles containing an ion complex of alginate–chitosan for designing a dry-coated tablet having a time-controlled releasing function. *Pharmaceutical Research, 17*, 94–99.

Vukanić, Z. S., Čolić, M., & Dimitrijević, M. (2007). Effect of pentoxifylline on differentiation and maturation of human monocyte-derived dendritic cells in vitro. *International Immunopharmacology, 7*, 167–174.

Xu, Z.-S., Yang, S.-H., Xiao, D.-M., Lin, B.-W., Zhang, X.-M., & Li, R. (2007). Effect of calcium alginate gel–bone morphogenetic protein–red bone marrow compound on the osteoinductivity. *Journal of Clinical Rehabilitative Tissue Engineering Research, 11*, 3640–3643.